INTERFACE

rsif.royalsocietypublishing.org

Research

Cite this article: Chaves LL, Lima S, Vieira ACC, Ferreira D, Sarmento B, Reis S. 2018 Overcoming clofazimine intrinsic toxicity: statistical modelling and characterization of solid lipid nanoparticles. *J. R. Soc. Interface* **15**: 20170932.
http://dx.doi.org/10.1098/rsif.2017.0932

Received: 11 December 2017
Accepted: 11 January 2018

Subject Category:
Life Sciences–Chemistry interface

Subject Areas:
nanotechnology, biomaterials

Keywords:
Box–Behnken design, cytotoxicity, leprosy, solubility

Author for correspondence:
Salette Reis
e-mail: shreis@ff.up.pt

Electronic supplementary material is available online at https://dx.doi.org/10.6084/m9.figshare.c.3991644.v1.

THE ROYAL SOCIETY PUBLISHING

Overcoming clofazimine intrinsic toxicity: statistical modelling and characterization of solid lipid nanoparticles

Luíse L. Chaves[1], Sofia Lima[1,2], Alexandre C. C. Vieira[1], Domingos Ferreira[3], Bruno Sarmento[2,4,5] and Salette Reis[1]

[1]LAQV, REQUIMTE, Departamento de Ciências Químicas, Faculdade de Farmácia, Universidade do Porto, Porto, Portugal
[2]CESPU, Instituto de Investigacão e Formação Avançada em Ciências e Tecnologias da Saúde and Instituto Universitário de Ciências da Saúde, Gandra, Portugal
[3]UCIBIO, REQUIMTE, Laboratório de Tecnologia Farmacêutica, Faculdade de Farmácia,
[4]I3S, Instituto de Investigacão e Inovação em Saúde, and [5]INEB – Instituto de Engenharia Biomédica, Universidade do Porto, Porto, Portugal

SL, 0000-0001-8777-5877; SR, 0000-0002-0736-2835

The aim of this work was to develop solid lipid nanoparticles (SLNs) loaded with clofazimine (CLZ) (SLNs-CLZ) to overcome its intrinsic toxicity and low water solubility, for oral drug delivery. A Box–Behnken design was constructed to unravel the relations between the independent variables in the selected responses. The optimized SLNs-CLZ exhibited the following properties: particle size *ca* 230 nm, zeta potential of −34.28 mV, association efficiency of 72% and drug loading of 2.4%, which are suitable for oral delivery. Further characterization included Fourier transformed infrared spectroscopy that confirmed the presence of the drug and the absence of chemical interactions. By differential scanning calorimetry was verified the amorphous state of CLZ. The storage stability studies ensured the stability of the systems over a period of 12 weeks at 4°C. *In vitro* cytotoxicity studies evidenced no effect of both drug-loaded and unloaded SLNs on MKN-28 gastric cells and on intestinal cells, namely Caco-2 and HT29-MTX cells up to 25 μg ml^{-1} in CLZ. Free CLZ solutions exhibited IC_{50} values of 16 and 20 μg ml^{-1} for Caco-2 and HT29-MTX cells, respectively. It can be concluded that the optimized system, designed considering important variables for the formulation of poorly soluble drugs, represents a promising platform for oral CLZ delivery.

1. Introduction

Clofazimine (CLZ) is an antibiotic and an anti-inflammatory drug, classified as a riminophenazine agent [1,2]. For decades, it has been recommended by the World Health Organization for the therapy of multibacillary leprosy. In addition, recent studies have revised its application in the treatment of multidrug-resistant tuberculosis [1,2].

Despite its clinical approval, it is a highly hydrophobic drug (log $p > 7$) [1], virtually insoluble in water [2]. This particular feature of CLZ results in limited absorption, associated with a large volume of distribution and, an elimination half-life of more than 70 days, since cells act as drug reservoirs [3]. After long-term administration, the consequent bioaccumulation of CLZ results in yellowish and reddish skin pigmentation, abdominal pain and cardiotoxicity [1].

CLZ has three amine groups, which may be protonated and charged at acidic pH, increasing its solubility. Therefore, in the gastrointestinal tract, CLZ may form supersaturated solutions, as it passes from the stomach (pH 1–3) [4] to more alkaline environment of the intestine leading to *in vivo* drug precipitation [2]. In fact, it is already reported that CLZ can form complexes with intracellular membranes, and precipitate as crystal aggregates, being phagocytized by the mononuclear phagocyte system [2]. This phenomenon may be correlated with

Table 1. Formulation composition and obtained responses of 15 different formulation obtained from Box–Behnken design. X_1 = amount of lipid, X_2 = amount of surfactant, X_3 = amount of drug, Y_1 = particle size, Y_2 = PDI, Y_3 = zeta potential, Y_4 = AE and Y_5 = DL.

	independent variables			dependent variables				
formulation	X_1 (mg)	X_2 (mg)	X_3 (mg)	Y_1 (nm)	Y_2	Y_3 (mV)	Y_4 (%)	Y_5 (%)
F1	250	60	7	208.0	0.127	−28.04	67.8	1.88
F2	350	60	7	236.5	0.158	−32.31	61.9	1.26
F3	250	100	7	169.0	0.174	−23.17	67.0	1.85
F4	350	100	7	195.0	0.158	−23.62	62.4	1.57
F5	250	80	4	198.1	0.164	−30.88	70.8	1.10
F6	350	80	4	227.1	0.169	−29.08	83.0	0.94
F7	250	80	10	204.3	0.165	−25.73	62.4	2.26
F8	350	80	10	221.2	0.156	−21.78	81.7	2.02
F9	300	60	4	203.3	0.193	−27.18	62.7	0.81
F10	300	100	4	187.0	0.168	−38.28	77.4	0.97
F11	300	60	10	220.7	0.154	−29.61	75.0	2.39
F12	300	100	10	177.5	0.154	−24.65	69.5	2.24
F13	300	80	7	227.2	0.155	−32.09	71.2	1.63
F14	300	80	7	219.7	0.194	−29.93	80.6	1.87
F15	300	80	7	219.7	0.147	−28.52	74.7	1.61

undesired and toxicological effects, often resulting in patients' non-compliance with treatment [5].

Several strategies are commonly applied to improve poorly soluble drugs solubility namely prodrug formation, salt formation [6], complexation with cyclodextrins [3] or other macromolecules [1,7], formulation of amorphous dispersions [8], use of co-solvents or surfactants [9], formulation of liposomes [10] and nanosuspensions [11]. Although many types of nanoparticles are available for oral delivery, lipid nanoparticles and especially solid lipid nanoparticles (SLNs), have shown to be one of the most promising delivery systems to improve the oral bioavailability of hydrophobic drugs [12].

SLNs consist of a physiological compatible solid lipid core and of an amphiphilic surfactant shell. The main characteristic of the lipid phase is that they remain in solid state at room temperature [13,14]. The mechanism by which SLNs can improve the solubility of poorly soluble drugs is based on the formation of a fine lipid dispersion, at the same time that entraps the drug, providing a large surface area of absorption in the gastrointestinal tract [15]. Besides the traditional advantages of colloidal systems such as improved physical stability, protection of drug from *in vivo* degradation, controlled drug release, and specific targeting, SLNs are feasible to scale-up with an associated low cost [12,13].

Despite the great number of works applying different technologies to improve CLZ solubility, the encapsulation into SLNs has not yet been described. The aim of this work was to develop SLNs loaded with CLZ (SLNs-CLZ) to improve CLZ solubility, and to decrease its associated toxicity, using a rational development. The design of the SLNs-CLZ was carried out by the application of a Box–Behnken design (BBD) aiming to better unravel the influence of different factors on selected responses. The optimized formulations were physicochemically characterized by dynamic light scattering, Fourier transformed infrared spectroscopy, differential scattering calorimetry. The storage stability and the *in vitro* cytotoxicity were also assessed.

2. Material and methods

2.1. Materials

CLZ was purchased from Hangzhou Heta Pharm & Chem Co. The solid lipids Precirol ATO 5 cetyl palmitate, Compritol 888 ATO, Precirol ATO 5, Gelucire 43/01, were kindly provided by Gattefossé (Saint-Priest, France). Softisan 142 was purchased from Cremer Care (Hamburg, Germany); Witepsol E85 from Sasol (Johannesburg, South Africa), and stearic acid was from Merck & Co., Inc. (Whitehouse Station, NJ, USA). Tween® 80 was purchased from Sigma-Aldrich Co. (St Louis, MO, USA). All other chemicals used in the study were of analytical grade. Caco-2 and MKN28 cell lines were acquired from the Shanghai Institute of Cell Biology (Shanghai, China) (passage number 35–55); while the HT29-MTX cell line was kindly provided by Dr T. Lesuffleur (INSERM U178, Villejuif, France). Dulbecco's modified Eagle's medium (DMEM), Roswell Park Memorial Institute (RPMI), fetal bovine serum (FBS), Pen-Strep (penicillin, streptomycin) and trypsin-EDTA were all obtained from Gibco (Paisley, UK). Thiazolyl blue tetrazolium bromide (MTT) was obtained from Sigma-Aldrich (St Louis, MO, USA).

2.2. Methods

2.2.1. Preparation of SLNs

All the formulations of the experimental design were prepared by hot homogenization followed by ultrasonication, as previously described [14]. Briefly, the selected amounts of Precirol ATO 5 and CLZ (table 1) were both heated to 75°C to solubilize the drug in the lipid matrix. Further, the aqueous phase containing the established amount of surfactant (Tween® 80) (table 1) was pre-heated in water bath at the same temperature. The 6 ml of aqueous phase were added into the lipid phase and homogenized

using a probe sonicator (VCX130; Sonics & Materials, Inc., Newtown, CT, USA), at 70% of amplitude for 5 min. The colloidal dispersion obtained was rapidly cooled down in an ice bath. Placebo SLNs were prepared similarly, without the addition of CLZ. When appropriate, the formulation was freeze-dried for 48 h, under vacuum (0.5 mBar), and −55°C using a LyoQuest 85 plus v.407 Telstar freeze dryer (Telstar® Life Science Solutions, Terrassa, Spain).

2.2.2. Experimental design

In order to assess the correlation between the responses and the factors during the development of SLNs-CLZ, maximizing the experimental efficiency with the minimum number of experiments, a three-level, three-factor BBD was applied.

The selected independent variables were (X_1) the amount of lipid, (X_2) the amount of surfactant and (X_3) the amount of drug. These parameters and their lower (−1), medium (0) and higher (+1) values were selected based on previous screening studies for each variable. Other parameters were set as fixed levels. The studied responses were: Y_1 = mean particle diameter, Y_2 = polydispersity index (PDI), Y_3 = zeta potential (ZP), Y_4 = association efficiency (AE) and Y_5 = drug loading (DL). The results were studied using analysis of variance (ANOVA). Multiple linear regression analysis of the BBD was carried out to generate polynomial equations

$$Y = b_0 + b_1X_1 + b_2X_2 + b_3X_3 + b_{12}X_1X_2 + b_{13}X_1X_3 + b_{23}X_2X_3 + b_{11}X_{1^2} + b_{22}X_{2^2} + b_{33}X_{3^2},$$

where Yn is response b_0 is the arithmetic mean of all the runs, X_{1-3} are the coded levels of independent variables, and b_1–b_{33} are the estimated coefficient from the observed experimental values of the respective response (Yn); the terms $XiXj$ and X_{i2} ($i = 1$, 2 or 3) represent the interaction and quadratic terms, respectively. A positive sign of the terms indicates synergic effects of the factors, while negative signs indicate antagonistic effect.

The best-fitting experimental model (linear, two-factor interaction, quadratic, and cubic models) was statistically evaluated according to multiple correlation coefficient (R^2) provided by STATISTICA 10 software (StatSoft®, Dell Software, Round Rock, TX, USA). The effects of the obtained models were assessed by analysing the statistical significance of the coefficients using ANOVA (p-value 0.05).

2.2.3. Optimization and validation assays

The optimization of the formulation was performed assuming the values obtained after studying the desirability profile tool of STATISTICA 10 software. The constraints parameters were to: reach particles with 250 nm in diameter, minimize PDI, obtain a charge around −30 mV, and maximize AE and DL, all simultaneously. Three-dimensional response surface plots were obtained for each response in order to better understand the correlation between the factors.

To evaluate the reliability of the models, the optimized nanoparticle was used as check point for the validation, in which the predicted values of each response were compared to the experimental by calculating the % bias. The linear correlation and residual plots between observed and predicted responses were obtained. The optimized nanoparticles were used for the subsequent characterization.

2.2.4. Characterization of the optimized SLNs-CLZ

2.2.4.1. Mean particle size, polydispersity index and zeta potential

The mean particle size as well as the PDI were analysed by dynamic light scattering (DLS) using a ZetaPALS, Zeta Potential Analyzer (Brookhaven Instrument Corps, Holtsville, NY, USA), at 25°C with a light incidence angle of 90°.

Before measurement, the formulation was filtered with a nitrocellulose 3 µm pore size filter (Merck Millipore, Billerica, MA, USA), aiming to exclude the unentrapped precipitated drug. Further, the filtrated nanoparticles were properly diluted with ultrapure water until reaching a suitable concentration for the measurement, that is, Kcps around 500. The obtained values of particle size and PDI were representative of the mean of six runs. The zeta potential of the samples was analysed by electrophoretic light scattering (ELS) using the Smoluchowski mathematical model. The filtered nanoparticles were measured in a folded capillary electrophoresis cell, at 25°. The obtained value represents the mean of multiple runs ($n = 10$).

2.2.4.2. Association efficiency and drug loading

The quantification of entrapped drug within the SLNs was carried out based on methodologies already reported [16]. Briefly, fresh optimized formulation was filtered through a 3 µm nitrocellulose membrane filter (Merck Millipore, Billerica, MA, USA) to retain unentrapped drug crystals which were undissolved. The drug retained in the filter was recovered with HCl 1 M, and the amount of free CLZ was measured by UV-Vis spectrophotometer (Jasco V-660, Easton, MD, USA) at 528 nm. The method for CLZ quantification in nanoparticles formulations was previously developed and validated (electronic supplementary material, figure S1 and supplementary material). The amount of soluble drug in the aqueous phase was determined by the ultrafiltration method. Briefly, SLNs-CLZ was properly diluted in ultrapure water, then transferred into Amicon® Ultra-4 Centrifugal Filter Devices (Millipore, Billerica, MA, USA) (molecular weight cut-off 50 K), and centrifuged using an Allegra X-15R centrifuge (Beckman Coulter, Brea, CA, USA) at 4000g for 10 min. After centrifugation, the samples were acidified with HCl until reaching the concentration of 1 M, and the free CLZ was detected by spectrophotometer at 528 nm. Standard curves were obtained in HCL 1 M and the supernatant of the aqueous phase solution obtained after Amicon filter centrifugation, used to determine the CLZ concentration. The results are expressed as mean ± standard deviation ($n = 3$). Association efficiency (AE) was calculated following the equation:

$$\mathrm{AE} = \frac{\text{initial amount of drug} - (\text{drug retained in filter 3 µm} + \text{drug soluble in aqueous phase})}{\text{initial amount of drug}} \times 100.$$

Drug loading (DL) expresses the per cent of drug entrapped in relation to the total lipids and excipients.

$$\mathrm{DL} = \frac{\text{initial amount of drug} - \text{recovered drug}}{\text{total weight of nanoparticles}} \times 100.$$

2.2.4.3. Freeze-drying of optimized SLNs-CLZ

Optimized SLNs-CLZ underwent freeze-dried filtration using a 3 µm nitrocellulose membrane filter (Merck Millipore, Billerica, MA, USA) to retain unentrapped drug crystals. The samples were freeze-dried (Lyoquest ECO, Telstar) with no cryoprotector, using

a condenser temperature of −65°C and pressure of 0.5 mbar, during 48 h. The samples were stored in desiccator until further use.

2.2.4.4. Transmission electron microscopy to assess morphology

The morphology of the freeze-dried SLNs-CLZ was observed by TEM (TEM Jeol JEM-1400; JEOL Ltd, Tokyo, Japan) analysis. After nanoparticles hydration with double-deionized water, one drop of nanoparticle suspension was added to a copper grid. The images were obtained after negative staining with uranyl acetate and under an accelerating voltage of 60 kV.

2.2.4.5. Fourier transform infrared spectroscopy

Fourier transform infrared spectroscopy (FTIR) spectra of CLZ, Precirol ATO 5 and CLZ physical mixture (PM), and freeze-dried SLNs and SLNs-CLZ were using a PerkinElmer® Spectrum 400 (Waltham, MA, USA) equipped with an attenuated total reflectance (ATR) device and zinc selenite crystals. The samples were transferred directly to the ATR compartment, and the result was obtained by combining the 16 scans. The spectra were recorded between 4000 and 600 cm^{-1} with a resolution of 4 cm^{-1}.

2.2.4.6. Differential scanning calorimetry

Differential scanning calorimetry (DSC) thermal analyses of CLZ, Precirol ATO 5, PM, freeze-dried SLNs and SLNs-CLZ were performed using a DSC 200 F3 Maia (Netzsch, Selb, Germany). Briefly, accurately weighted samples (1–2 mg) were poured into aluminium pans and hermetically sealed. An empty pan was used as reference. The samples were scanned from 30 to 300°C, at 10°C min^{-1} of flow rate. Nitrogen gas was used as purge gas, at 40 ml min^{-1}. The melting point (peak maximum), was calculated using the (NETZSCH Proteus® Software—Thermal Analysis—Version 6.1) software provided for the DSC equipment.

2.2.5. Storage stability studies

The storage stability of the SLNs-CLZ nanoparticles was assessed by conducting a study for a period of 12 weeks, at 4°C. At each time point, the formulation was characterized regarding particle size, PDI, zeta potential, AE and DL. The results were compared to the first day of production.

2.2.6. Cell-SLNs interaction studies

Intestinal Caco-2 and HT29-MTX cells were cultured in DMEM supplemented with 10% (v/v) of FBS and 1% (v/v) of penicillin–streptomycin. Gastric MKN-28 cells were cultured in RPMI 1640 culture medium, with 10% (v/v) FBS and 1% (v/v) of penicillin–streptomycin. Cells were grown in a humidified incubator at 37°C and 5% CO_2 atmosphere and 95% relative humidity. To detached the cells, a 0.25% (w/v) trypsin–EDTA solution was used when cells' confluence reached 80%

The potential cell cytotoxicity of SLNs, SLNs-CLZ and CLZ pure drug was evaluated against Caco-2, HT29-MTX and MKN-28 cells lines using the 3-(4, 5-dimethylthiazol-2-yl)-2,5-diphenyltetrazolium bromide (MTT) colorimetric assay. Separately, each cell line was transferred into 96-well plates, at a density of 5×10^4 cells per well for Caco-2 and HT29-MTX and 10^5 cells per well for MKN-28 cells. The plates were incubated for 18–24 h for cell attachment. Further, the culture media was removed and the wells were incubated with 100 µl of culture media containing different concentrations of SLNs, SLNs-CLZ and CLZ (6.25–50 µg ml^{-1} equivalent of CLZ). For CLZ pure drug, the samples were prepared from a stock solution in DMSO, and appropriate dilutions were done to reach maximum of 4% (v/v) of DMSO in the well, immediately before the beginning of the assay. Each sample was incubated during 24 h for Caco-2 and HT29-MTX cell lines; and during 4 h for MKN-28. After the incubation period, the samples were removed and replaced by 100 µl of MTT solution (0.5 mg ml^{-1}), and incubated for additional 2 h. Further, the MTT solution was removed and 100 µl of DMSO was added into each well to solubilize the formazan crystals. The optical density of the solution was measured at 570 and 630 nm wavelengths using Synergy™ HT Multi-mode microplate reader (BioTek Instruments Inc., Winooski, VT, USA). Untreated cells were taken as positive control with 100% viability and cells incubated with 4% (v/v) DMSO used as control for free CLZ. The MTT test was performed in triplicate and results were expressed as mean values ± standard deviation (s.d.). The cell viability (%) in relation to control cells (untreated cells) as follows:

$$\text{cell viability (\%)} = \frac{\text{OD570} - 630 \text{ treated cells}}{\text{OD570} - 630 \text{ untreated cells}} \times 100.$$

2.2.7. Statistical analysis

All results were expressed as mean ± s.d. ($n = 3$). The method validation was carried out using ANOVA, regression analysis, and Student's *t*-test. Data obtained from the experimental design were analysed by ANOVA and multiple correlation coefficient using STATISTICA 10 (StatSoft®) software. GraphPad Prism software (version 6, GraphPad Software, USA) was used for statistical comparisons of the results to control for the cytotoxicity, through Student's (unpaired) *t*-test and one-way ANOVA test. The differences were assumed statistical significant when $p < 0.05$ (95% confidence level).

3. Results and discussion

3.1. Experimental design

The significance of the screened factors was assessed and then an experimental design was constructed with the identified variables that may influence the critical attributes of the SLNs. In this context, (X_1) amount of lipid, (X_2) amount of surfactant and (X_3) amount of drug were used to explore individual and synergic effects on the particle size, polydispersity index (PDI), zeta potential, association efficiency (AE) and drug loading (DL).

The lower (−1), medium (0) and higher values (+1) for the factors were set out according to preliminary studies and literature research. A three-level, three-factor BBD was applied to optimize SLNs, allowing maximizing the experimental efficiency, with a minimum number of experiments. Fifteen formulations were prepared and analysed regarding the adopted responses. The experimental design included three replicates of the central point aiming to estimate the experimental error and accurately test the fit of the model. The data obtained are expressed in table 1.

The effects of the factors coefficients were evaluated via regression analysis for each independent variable, which were considered statistically significant when *p* values were less than 0.05, with 95% of confidence level. Because all the PDI values were below 0.2, which is considered to be a homogeneous dispersion, this response was not statistically evaluated.

The polynomial equation generated after fitting in second-order quadratic models showed good correlations (R^2) after multiple linear regression analysis for all the responses (table 2), with insignificant lack of fit. Moreover, the significance of the obtained models was tested by ANOVA, and tested by evaluating *p* values. All the mathematical models were considered precise in the prediction of the respective response as all the *p* values where 0.05.

Table 2. Summary of the regression analysis of the independent variables Y_1-Y_4. X_1 = amount of lipid, X_2 = amount of surfactant, X_3 = amount of drug, β_0 = arithmetic mean of all runs. Bold values represent coefficients with $p < 0.05$.

	particle size (Y_1)		zeta potential (Y_2)		EE (Y_3)		DL (Y_4)	
	coefficient	*p*-value	coefficient	*p*-value	coefficient	*p*-value	coefficient	*p*-value
β_0	203.975	**0.000**	−27.861	**0.000**	70.121	**0.000**	1.681	**0.000**
X_1	12.908	**0.015**	−0.308	0.691	0.868	0.671	−0.190	**0.044**
X_1^2	1.131	0.421	−1.614	0.075	1.860	0.269	0.015	0.653
X_2	−18.375	**0.008**	1.748	0.121	0.723	0.721	0.053	0.327
X_2^2	8.906	**0.016**	−0.083	0.875	3.513	0.104	0.043	0.270
X_3	0.708	0.704	3.008	**0.046**	−1.238	0.555	0.704	**0.003**
X_3^2	3.631	0.084	−0.042	0.937	−1.341	0.389	0.002	0.953
X_1X_2	−0.625	0.800	0.955	0.399	0.337	0.900	0.089	0.248
X_1X_3	−1.075	0.555	1.309	0.176	5.236	0.088	0.077	0.187
X_2X_3	2.625	0.229	−2.463	0.061	1.187	0.551	−0.037	0.441
	$R^2 = 0.993$		$R^2 = 0.975$		$R^2 = 0.940$		$R^2 = 0.995$	

3.1.1. Effect on mean particle size

The size of the nanoparticles is an important parameter to control during the nanoparticle formulation as it seems to influence *in vivo* distribution, biological fate, toxicity and drug loading capacity [17].

The obtained values of particle size from the formulations generated by the BBD ranged from 169.0 nm (F3) to 236.5 nm (F2), with a mean size (β_0) of 204.0 nm (table 1). According to the regression analysis (table 2), the amount of lipid (X_1) and the amount of surfactant (X_2) seemed to statistically influence SLN particle size, as they presented p values < 0.05, with 95% of confidence level. The positive sign of the X_1 coefficient reveals that the size increases with increasing amounts of lipid. On the contrary, the negative sign before the coefficients shows that higher amounts of surfactant (X_2) result in smaller particles. Also, the significance of the X_2 quadratic coefficient evidences a nonlinear relation of the response (particle size) with the changing of the values.

3.1.2. Effect on zeta potential

The zeta potential measures the electric charge present on the surface of the particles. This parameter is associated with colloidal stability so that generally, the greater the zeta potential the more likely the suspension is to be stable as the charged particles repel one another, overcoming the tendency to aggregate. It is currently admitted that zeta potentials of |30| mV are required for full electrostatic stabilization [18].

The zeta potential measured from the 15 formulations ranged from −21.78 mV (F8) to −38.28 mV (F10) (table 1). Only the amount of drug (X_3) seemed to affect the surface charge of the nanoparticles (p value 0.046), with 95% of confidence level (table 2). The positive sign of the coefficient means that the zeta potential increases with the augment of the amount of CLZ. The zeta potential is expressed as negative values, so that the higher the value, the closer it is to neutral.

In this case, it seems that the excess of CLZ may neutralize the surface charge of the nanoparticles, as it may be localized in the outer portion of the nanoparticle, thus influencing the surface charge.

3.1.3. Effect on drug association efficiency

The association efficiency (AE) is one of the most critical attribute when designing nanoformulations as high values of AE improves formulation yield. This fact is even more important when the drug presents severe adverse side effect, as is the case of CLZ. Drug entrapment inside nanoparticles depends on the solubility of the drug in the solid lipid and on the O/W partition of the drug.

The AE values of all the 15 formulations are shown in table 1. In general, all the formulations presented satisfactory AE values, ranging from 61.9% (F2) to 83.0% (F6), with a mean value (β_0) of 70.121% (table 1). The regression analyses evidenced that none of the variables influenced statistically the percentages of drug AE (table 2). Considering the high values and narrow range of AE percentages, this result may not be considered as negative as the selected levels used for all the variables originated suitable formulations in terms of AE.

3.1.4. Effect on drug loading

During the development of any nanoformulations, high values for drug loading (DL) are preferred as it means less carrier materials and excipients will enter the patient's body, leading to lower risks of toxicity [12].

The DL obtained from the 15 formulations ranged from 0.81% (F9) to 2.39% (F11) (table 1). The regression analysis of the model showed that the DL statistically alters with the changing of (X_1) the amount of lipid, and (X_3) the amount of drug, with 95% of confidence level (table 2). The negative sign of the X_1 coefficient demonstrates the inverse relation between the amount of lipid and DL, i.e. DL decreased with increasing amounts of lipid. The opposite is observed with increasing amounts of drug, as the sign is positive. The result is in accordance with the mathematical equation for the calculation of DL (§2.2.4.2).

Although this result seems to be obvious, it is not a rule, mainly in the case of very poorly water soluble drugs such as CLZ. The DL is a parameter related to the distribution of the drug between the lipid and aqueous phases, which is

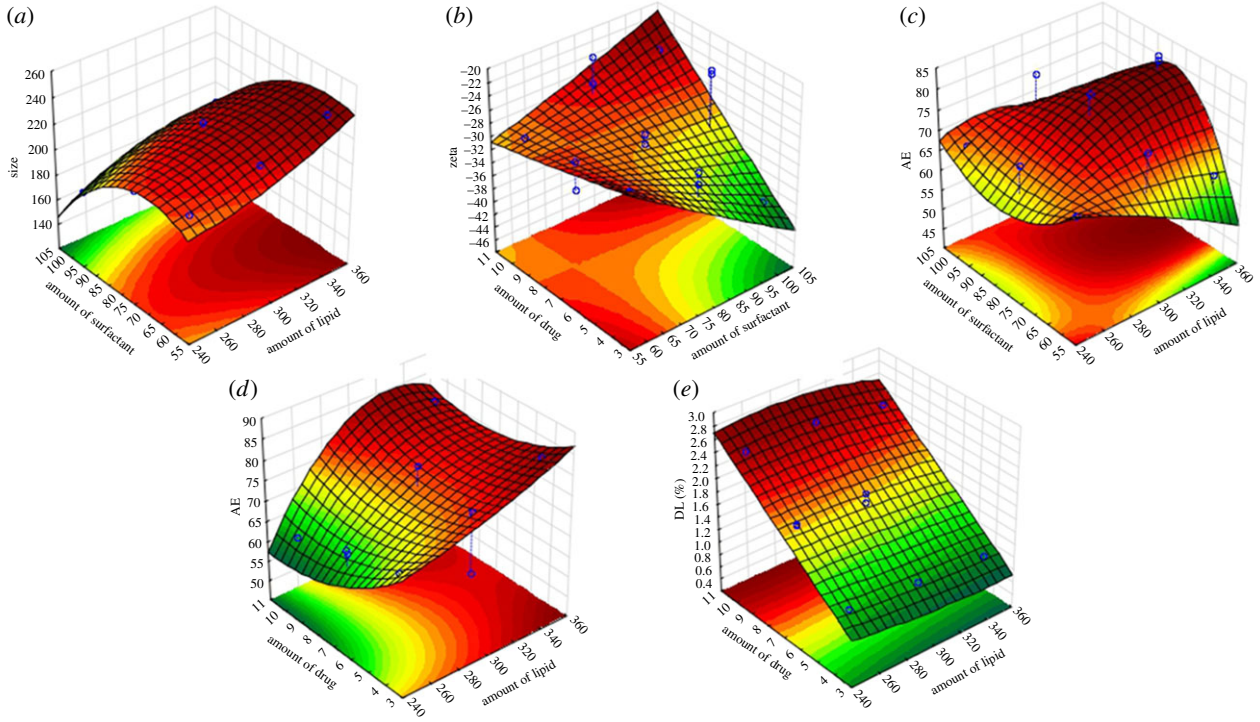

Figure 1. Response surface plots evidencing the influence of the independent variables on the selected responses particles size (Y_1) (*a*), zeta potential (Y_2) (*b*), AE (Y_3) (*c*,*d*) and DL (Y_4) (*e*). (Online version in colour.)

Table 3. Summary of the coded levels of the Box–Behnken design; the levels of the optimized formulation, the desirable parameters used for the optimization, and the comparison between predicted and observed values for the considered responses.

factors	coded levels			
independent variables	**low level (−1)**	**medium level (0)**	**high level (+1)**	**optimized**
X_1 = amount of lipid (mg)	250	300	350	300 mg
X_2 = amount surfactant (mg)	60	80	100	60 mg
X_3 = amount of drug (mg)	4	7	70	10 mg
dependent variables	**constraints**	**predicted**	**observed**	**bias[a]**
Y_1 = particle size (nm)	optimum (250 nm)	233	230	1.45
Y_2 = zeta potential (mV)	<-30	−32.59	−34.28	4.93
Y_3 = association efficiency	maximum	69%	72%	3.93
Y_4 = drug loading	maximum	2.44%	2.32	5.23

[a]Bias (%) = |predicted − observed|/observed × 100.

determined by the drug's solid-state nanocarrier matrix [12]. If the amount of lipid is not enough to solubilize the selected amount of drug, thus this relation would be not so predictable. In this case, this critical step was overcome by evaluating previously the solubility of CLZ in Precirol ATO 5 during the pre-formulation studies.

3.1.5. Optimization of SLNs-CLZ

After the evaluation of the relationships between factors and responses by the polynomial equations, the optimization of the formulation was carried out. Three-dimensional response surface analyses were plotted to provide a graphical representation of the behaviour of each response with the simultaneous changing of two factors at a time, maintaining non-used variables fixed at their middle level (figure 1). Furthermore, the optimization of SLNs-CLZ was carried out using the desirability function of the STATISTICA10 software [19]. This approach is a useful tool to overcome the difficulties of multiple or opposite optimal values for the different responses, as each response is associated with its own partial desirability function. The optimal nanoparticles had to satisfy the selected requirements for each dependent variable, namely nanoparticles with size closer to 250 nm, zeta potential closer to −30 mV, maximum AE and DL. The optimal calculated levels are expressed in table 3.

The qualities of the models were assessed by plotting predicted versus of the experimental data (electronic

supplementary material, figure S2 and supplementary material), confirmed by the low mean percentage of bias (table 3).

The validation of the models was performed by formulating the optimized formulation with (X_1) 300 mg of lipid, (X_2) 60 mg of surfactant and (X_3) 10 mg of CLZ. The check point responses were then estimated by the mathematical models and the experimental data were compared with the predicted. The lower magnitude of the bias reveals good correlation of the models, and is indicative of the robustness and high predictive ability of the mathematical models.

3.2. Characterization of the optimized SLNs-CLZ

3.2.1. Measurement of mean particle size, polydispersity index and zeta potential

The obtained nanoparticles presented a size of 230.0 ± 8.3 nm which was very close to the desired value of 250.0 nm; suitable PDI below 0.200 (0.149 ± 0.010) and zeta potential closer to −30 mV (−34.28 ± 2.80 mV). Unloaded SLNs were also prepared and values of 216.8 ± 16.5, 0.166 ± 0.020 and −32.23 mV for particle size, PDI and zeta potential respectively, evidenced that particles were similar to SLNs-CLZ.

3.2.2. Association efficiency and drug loading determination

The determination of AE and DL of SLNs-CLZ was performed in triplicate and the values obtained were 71 ± 2% and 2.4 ± 0.1% respectively. The results obtained were considered satisfactory taking into account the issues during the pre-formulation studies namely the poor solubility of CLZ in aqueous phase and even in the molten lipid.

3.2.3. Morphology evaluation

TEM images of the optimized SLNs-CLZ were obtained to investigate structural and morphological features of the nanoparticles. Figure 2 images revealed that the lipid nanoparticles were spherical in shape and that the nanoparticles presented a narrow diameter distribution with particle diameter near 250 nm, in accordance with the DLS measurement (table 3). Some unshaped matter is also observed in the TEM image, probably related to the freeze drying process, as lipid nanoparticles maybe disrupted during the freezing [20]. The presence of regular particles, the absence of any crystal matter and of particle aggregation corroborate the PDI results, showing only one nanoparticle's population.

3.2.4. SLNs-CLZ characterization by Fourier transform infrared spectroscopy

The FTIR spectra of CLZ, physical mixture (PM), SLNs and SLNs-CLZ are shown in figure 3. Both SLNs and SLNs-CLZ displayed typical bands at 2820 cm^{-1} and 1705 cm^{-1} relative to C–H and C=O (carbonyl) stretching of glyceryl units, respectively. The spectrum of CLZ present characteristic bands of N–H bending frequency at 1550−1620 cm^{-1}, and another regarding C=N stretching at 1625 cm^{-1} [6]. Unknown peaks were not found in the spectra, confirming that there is no chemical interaction between CLZ and SLNs constituents. Due to the amorphous state of entrapped CLZ, the intensity of characteristic peaks may be decreased and/or overlapped by others belonging to the major constituents of SLNs-CLZ.

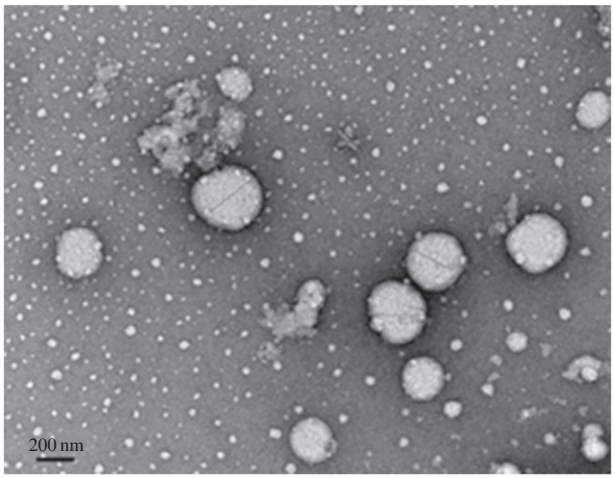

Figure 2. TEM image of optimized SLNs-CLZ, amplification 50 000×.

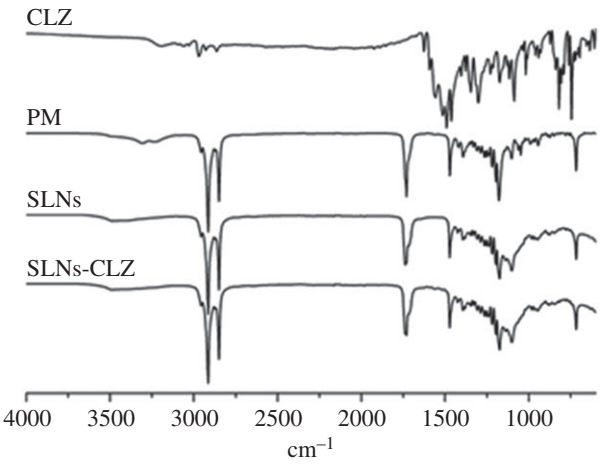

Figure 3. FTIR spectra of CLZ, physical mixture (PM), SLNs and SLNs-CLZ.

3.2.5. Assessment of CLZ physical state in the SLNs by differential scanning calorimetry

Differential scanning calorimetry (DSC) studies were conducted to study the physical state of CLZ in the nanoparticles, identify potential Precirol ATO 5-CLZ interactions during the production process and to evaluate the behaviour of the lipid phase.

The thermograms of CLZ, Precirol ATO 5, PM, SLNs and SLNs-CLZ can be observed in figure 4. The endothermic event of CLZ at 224°C was not observed in SLNs-CLZ, which suggests that CLZ is encapsulated in amorphous form in nanoparticle formulation. Similar results were observed with Precirol ATO 5 and poorly soluble compounds [16,21]. Furthermore, no additional unknown peaks were found, indicating no incompatibility between Precirol ATO 5 and CLZ.

Precirol ATO 5 thermograms shows an endothermic event at 58°C with a shoulder at 62°C, characteristic of the diffuse melting in complex glycerides due to the presence of different polymorphs (figure 3) [22]. This phenomenon was not observed in both loaded and unloaded nanoparticles, which may suggest that the lipids undergo some polymorphic changes to less ordered structures during particle preparation allowing better incorporation of the drug in the lipid matrix [23].

In the PM, the onset temperature of this event shifted to lower temperature, indicating that the presence of CLZ in the crystalline form interfered in the lipid melting. This

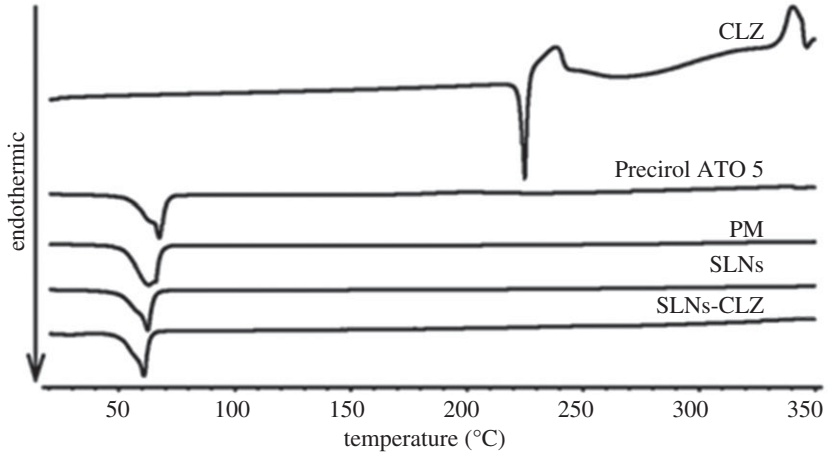

Figure 4. DSC thermograms of CLZ, physical mixture (PM), Precirol ATO 5, SLNs and SLNs-CLZ.

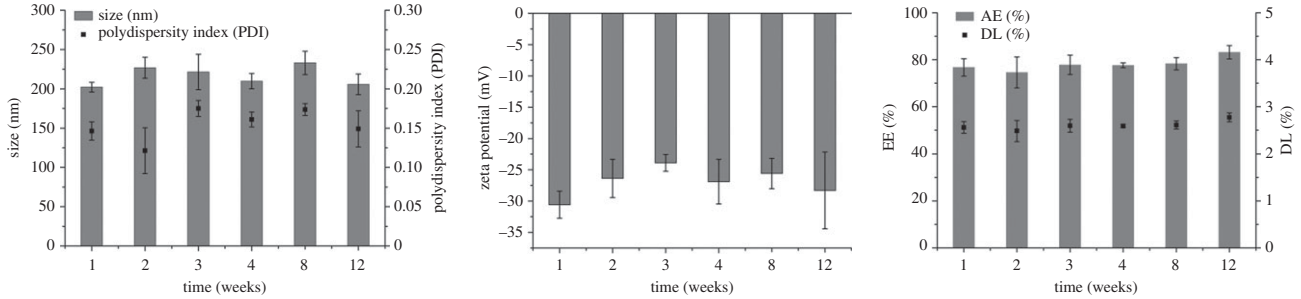

Figure 5. Storage stability at 4°C assessed as (*a*) particle size as bars and PDI as black circles, (*b*) zeta potential, (*c*) drug content of SLNs-CLZ expressed as AE (bars) and DL (circles) (mean ± s.d., $n = 3$).

shifting in Precirol ATO 5 onset melting temperature was not observed for both SLNs and SLNs-CLZ. On the other hand, onset temperatures of lipid transition for both SLNs and SLNs-CLZ were quite similar suggesting that the presence of the drug did not alter the lipid conformation, probably because it is well dispersed. These findings were already reported to Precirol ATO 5 and other compounds [22].

Moreover, in the PM thermogram no endothermic event was found around 224°C, suggesting that CLZ was solubilized in the molten lipid which may be considered a positive interaction between lipid and drug due to the suitable solubility of CLZ in the selected lipid.

3.2.6. Storage stability studies

The physical stability of the optimized SLNs-CLZ was evaluated regarding particle size, PDI, zeta potential, AE and DL, upon storage of the colloidal suspensions at 4°C, during 12 weeks. Changes in particle size and PDI are indicators of formulation instability and the surface charge is commonly related to the aggregation of the particles [18].

Figure 5 shows the results obtained after each time point for the tested parameters. At the end of the study, no aggregation or colour change were found through visual observations. Moreover, the initial characteristics were maintained, with no significant changes ($p > 0.5$). Particles size varied about 30 nm from the initial values and PDI was always below 0.2. The colloidal suspensions remained with negative values closer to −30 mV, which indicate stable dispersion due to the electric repulsion between the particles. It was observed that the SLNs did not release CLZ over time at 4°C, as the AE and DL values were practically constant (figure 5*c*). This can be considered a positive result as it is common to observe drug expulsion after lipid crystallization upon storage [18]. Overall, the developed SLNs-CLZ was stable when stored at 4°C for 12 weeks.

3.2.7. *In vitro* cell viability studies

SLNs-CLZ development aims to provide oral drug delivery in leprosy therapy. Thus, different cell lines were selected as suitable models mimicking the different cell-types of the gastrointestinal tract (e.g. stomach, enterocytes and mucus secreting cells) [24,25]. Caco-2, HT29-MTX (intestinal model cells) and MKN-28 (gastric model cell) cell viability studies were conducted with SLNs and SLNs-CLZ, in addition to CLZ free drug solution.

The studies were performed with different concentrations of nanoparticles corresponding to 6.26 to 50 μg ml^{-1} in CLZ, equivalent to 0.25–2 mg ml^{-1}, in relation to the amount of lipid, during 24 h for Caco-2 and HT29-MTX, and 4 h for MKN-28. Cytotoxicity studies were also carried out with CLZ solutions up to 50 μg ml^{-1}. The results obtained show that for Caco-2 cells, only the highest tested concentration of SLNs-CLZ (50 μg ml^{-1} in CLZ, 2 mg ml^{-1} in lipid) presented cell viability statistically different from the control (figure 6). Unloaded nanoparticles were considered safe as at all tested concentrations the viability of the cells was superior to 80%. For HT29-MTX and MKN28 cell lines, neither SLNs nor SLNs-CLZ presented statistical significance when compared to the control. These results show that the nanoparticles were not toxic for the studied cell lines when compared to free CLZ solutions. In fact, for all the intestinal cell lines, exposure to free CLZ led to a significant reduction in cell viability, and the IC_{50} values determined were 16.3 and 20.3 μg ml^{-1} for Caco-2 and HT29-MTX, respectively. Moreover, the high

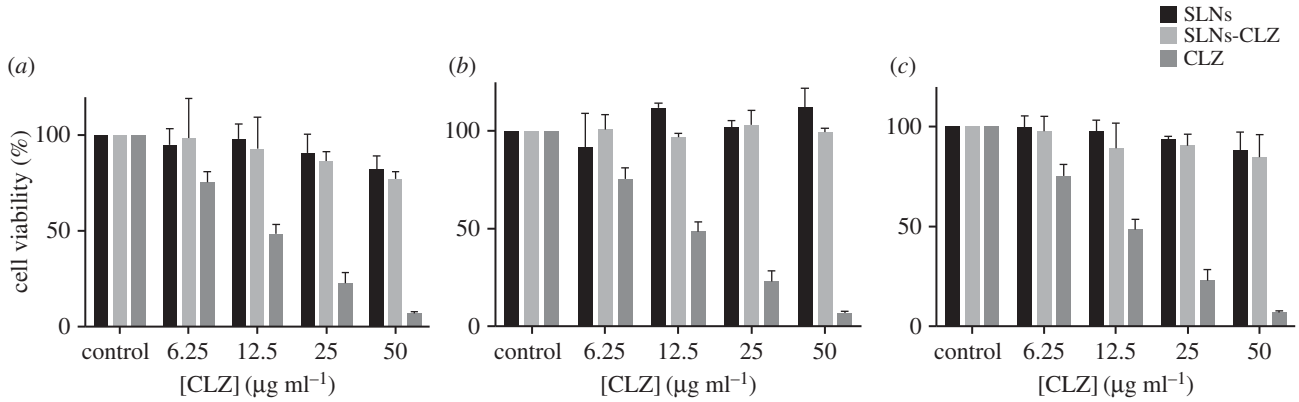

Figure 6. Cell viability of (*a*) MKN-28, (*b*) HT29-MTX and (*c*) Caco-2 cell lines upon exposure to SLNs (dark grey), SLNs-CLZ (light grey), and CLZ (grey). Data expressed as the average ± standard deviation ($n = 5$, for each three independent assays) (*p value <0.05 in relation untreated cells).

toxicity of CLZ has already been reported [26]. Upon prolonged oral administration, CLZ forms intracellular insoluble drug precipitates, leading to high concentration bioaccumulation, being easily associated with unwanted side effects such as reddish skin pigmentation, abdominal pain and cardiotoxicity [1].

Based on the exposed results, the successful incorporation of CLZ in SLNs, with the drug in its amorphous state, may prevent drug crystallization and the formation of precipitates *in vitro* and *in vivo*. In this context, the nanoformulations seem to have an elevated potential to delivery CLZ, decreasing the undesired effect, by protecting the surrounding cells from the toxic effects of the drug.

5. Conclusion

In the present study, a BBD was successfully obtained and the relations between the independent variables in the selected responses could be understood. The optimized SLNs-CLZ was achieved based on the desirability profile, which presented suitable parameters after characterization, namely particle size, zeta potential, AE and DL. FTIR confirmed the presence of the drug and the absence of chemical interactions, while DSC measurements indicated the amorphous state of CLZ when incorporated within the SLNs. The stability studies ensured that the developed SLNs are stable over a period of 12 weeks at 4°C. *In vitro* cytotoxicity studies evidenced that the optimized SLNs-CLZ are not toxic at the tested concentration range, contrary to CLZ solutions, which presented IC_{50} values around 20 μg ml^{-1} for Caco-2 and HT29-MTX cell lines.

Based on the results obtained, it can be concluded that the production of SLNs-CLZ was optimized, considering important variables for poorly soluble drugs and that solid lipid nanoparticles of Precirol ATO 5 are a promising platform to deliver CLZ with reduced associated effects.

Data accessibility. All supporting data are made available in the article.

Authors' contributions. L.L.C. prepared samples, performed the experiments, analysed the data, participated in the design of the study and drafted the manuscript; S.L. participated in the design of the work, helped with data analysis and drafted the manuscript; A.C.C.V. produced lipid nanoparticles and helped with sample preparation; D.F. participated in the design of the study and reviewed the manuscript; B.S. helped with data analysis and reviewed the manuscript; S.R. participated in the design of the study, analysed the data and drafted the manuscript. All the authors gave their final approval for publication.

Competing interests. We declare we have no competing interests.

Funding. This work received financial support from the European Union (FEDER funds) and National Funds (FCT/MEC, Fundação para a Ciência e Tecnologia and Ministério da Educação e Ciência) under the Partnership Agreement PT2020 UID/MULTI/04378/2013 - POCI/01/0145/FEDER/007728 and funds through the COMPETE 2020 - Operational Programme for Competitiveness and Internationalisation (POCI), Portugal 2020, and by Portuguese funds through FCT - Fundação para a Ciência e a Tecnologia/Ministério da Ciência, Tecnologia e Inovação in the framework of the projects 'Institute for Research and Innovation in Health Sciences' (POCI-01-0145-FEDER-007274).

Acknowledgements. S.L. thanks Operação NORTE-01-0145-FEDER-000011 for her Investigator contract. A.C.C.V. thanks the CNPq Foundation, Ministry of Education of Brazil for the Doctoral fellowship 246514/2012-4 and L.L.C. thanks the CAPES Foundation, Ministry of Education of Brazil for the Doctoral fellowship 0831-12-3.

References

1. Li S, Chan JY, Li Y, Bardelang D, Zheng J, Yew WW, Chan DP-C, Yuen Lee SM, Wang R. 2016 Complexation of clofazimine by macrocyclic cucurbit[7]uril reduced its cardiotoxicity without affecting the antimycobacterial efficacy. *Org. Biomol. Chem.* **14**, 7563–7569. (doi:10.1039/C6OB01060A)
2. Baik J, Rosania GR. 2012 Macrophages sequester clofazimine in an intracellular liquid crystal-like supramolecular organization. *PLoS ONE* **7**, e47494. (doi:10.1371/journal.pone.0047494)
3. Salem I, Steffan G, Düzgünes N. 2003 Efficacy of clofazimine-modified cyclodextrin against *Mycobacterium avium* complex in human macrophages. *Int. J. Pharm.* **260**, 105–114. (doi:10.1016/S0378-5173(03)00236-9)
4. Nunes R, Silva C, Chaves L. 2015 *Tissue-based* in vitro *and* ex vivo *models for intestinal permeability studies. Concepts and models for drug permeability studies: edition: cell and tissue based* in vitro *culture models*. Sawston, UK: Woodhead Publishing.
5. Yoon GS, Sud S, Keswani RK, Baik J, Standiford TJ, Stringer KA *et al.* 2015 Phagocytosed clofazimine biocrystals can modulate innate immune signaling by inhibiting TNFα and boosting IL-1RA secretion. *Mol. Pharm.* **12**, 2517–2527. (doi:10.1021/acs.molpharmaceut.5b00035)
6. Bolla G, Nangia A. 2012 Clofazimine mesylate: a high solubility stable salt. *Cryst. Growth Des.* **12**, 6250–6259. (doi:10.1021/cg301463z)
7. Hernandez-Valdepeña I, Domurado M, Coudane J, Braud C, Baussard J, Vert M, Domurado D. 2009

Nanoaggregates of a random amphiphilic polyanion to carry water-insoluble clofazimine in neutral aqueous media. *Eur. J. Pharm. Sci.* **36**, 345–351. (doi:10.1016/j.ejps.2008.10.008)

8. Nie H, Su Y, Zhang M, Song Y, Leone A, Taylor L, Marsac PJ, Li T, Byrn SR. 2016 Solid-state spectroscopic investigation of molecular interactions between clofazimine and hypromellose phthalate in amorphous solid dispersions. *Mol. Pharm.* **13**, 3964–3975. (doi:10.1021/acs.molpharmaceut.6b00740)
9. O'Reilly J, Corrigan O, O'Driscoll C. 1994 The effect of mixed micellar systems, bile salt/fatty acids, on the solubility and intestinal absorption of clofazimine (B663) in the anaesthetised rat. *Int. J. Pharm.* **109**, 147–154. (doi:10.1016/0378-5173(94)90142-2)
10. Patel V, Misra A. 1999 Encapsulation and stability of clofazimine liposomes. *J. Microencapsul.* **16**, 357–367. (doi:10.1080/026520499289077)
11. Peters K, Leitzke S, Diederichs JE, Borner K, Hahn H, Müller RH, Ehlers S. 2000 Preparation of a clofazimine nanosuspension for intravenous use and evaluation of its therapeutic efficacy in murine *Mycobacterium avium* infection. *J. Antimicrob. Chemother.* **45**, 77–83. (doi:10.1093/jac/45.1.77)
12. Narvekar M, Xue HY, Eoh JY, Wong HL. 2014 Nanocarrier for poorly water-soluble anticancer drugs—barriers of translation and solutions. *AAPS Pharm. Sci. Tech.* **15**, 822–833. (doi:10.1208/s12249-014-0107-x)
13. Righeschi C, Bergonzi M, Isacchi B, Bazzicalupi C, Gratteri P, Bilia A. 2016 Enhanced curcumin permeability by SLN formulation: The PAMPA approach. *Food Sci. Technol.* **66**, 475–483.
14. Vieira AC, Chaves LL, Pinheiro M, Ferreira D, Sarmento B, Reis S. 2016 Design and statistical modeling of mannose-decorated dapsone-containing nanoparticles as a strategy of targeting intestinal M-cells. *Int. J. Nanomed.* **11**, 2601–2617. (doi:10.2147/IJN.S117210)
15. Attama A, Umeyor C. 2015 The use of solid lipid nanoparticles for sustained drug release. *Ther. Deliv.* **6**, 669–684. (doi:10.4155/tde.15.23)
16. Das S, Ng WK, Kanaujia P, Kim S, Tan RB. 2011 Formulation design, preparation and physicochemical characterizations of solid lipid nanoparticles containing a hydrophobic drug: effects of process variables. *Colloids Surf. B Biointerfaces* **88**, 483–489. (doi:10.1016/j.colsurfb.2011.07.036)
17. Dhat S, Pund S, Kokare C, Sharma P, Shrivastava B. 2017 Risk management and statistical multivariate analysis approach for design and optimization of satranidazole nanoparticles. *Eur. J. Pharm. Sci.* **96**, 273–283. (doi:10.1016/j.ejps.2016.09.035)
18. Heurtault B, Saulnier P, Pech B, Proust JE, Benoit JP, Benoit JP. 2003 Physico-chemical stability of colloidal lipid particles. *Biomaterials* **24**, 4283–4300. (doi:10.1016/S0142-9612(03)00331-4)
19. Gupta B, Poudel BK, Pathak S, Tak JW, Lee HH, Jeong JH, Choi H-G, Yong CS, Kim JO. 2016 Effects of formulation variables on the particle size and drug encapsulation of imatinib-loaded solid lipid nanoparticles. *AAPS Pharm. Sci. Tech.* **17**, 652–662. (doi:10.1208/s12249-015-0384-z)
20. Choi MJ, Briançon S, Andrieu J, Min SG, Fessi H. 2004 Effect of freeze-drying process conditions on the stability of nanoparticles. *Drying Technol.* **22**, 335–346. (doi:10.1081/DRT-120028238)
21. Makled S, Nafee N, Boraie N. 2017 Nebulized solid lipid nanoparticles for the potential treatment of pulmonary hypertension via targeted delivery of phosphodiesterase-5-inhibitor. *Int. J. Pharm.* **517**, 312–321. (doi:10.1016/j.ijpharm.2016.12.026)
22. Fang J-Y, Fang C-L, Liu C-H, Su Y-H. 2008 Lipid nanoparticles as vehicles for topical psoralen delivery: solid lipid nanoparticles (SLN) versus nanostructured lipid carriers (NLC). *Eur. J. Pharm. Biopharm.* **70**, 633–640. (doi:10.1016/j.ejpb.2008.05.008)
23. Nafee N, Husari A, Maurer CK, Lu C, de Rossi C, Steinbach A, Hartmann RW, Lehr C-M, Schneider M. 2014 Antibiotic-free nanotherapeutics: ultra-small, mucus-penetrating solid lipid nanoparticles enhance the pulmonary delivery and anti-virulence efficacy of novel quorum sensing inhibitors. *J. Control Release* **192**, 131–140. (doi:10.1016/j.jconrel.2014.06.055)
24. Araujo F, Sarmento B. 2013 Towards the characterization of an *in vitro* triple co-culture intestine cell model for permeability studies. *Int. J. Pharm.* **458**, 128–134. (doi:10.1016/j.ijpharm.2013.10.003)
25. Fernandes I, de Freitas V, Reis C, Mateus N. 2012 A new approach on the gastric absorption of anthocyanins. *Food Funct.* **3**, 508–516. (doi:10.1039/c2fo10295a)
26. Arbiser JL, Moschella SL. 1995 Clofazimine: a review of its medical uses and mechanisms of action. *J. Am. Acad. Dermatol.* **32**, 241–247. (doi:10.1016/0190-9622(95)90134-5)